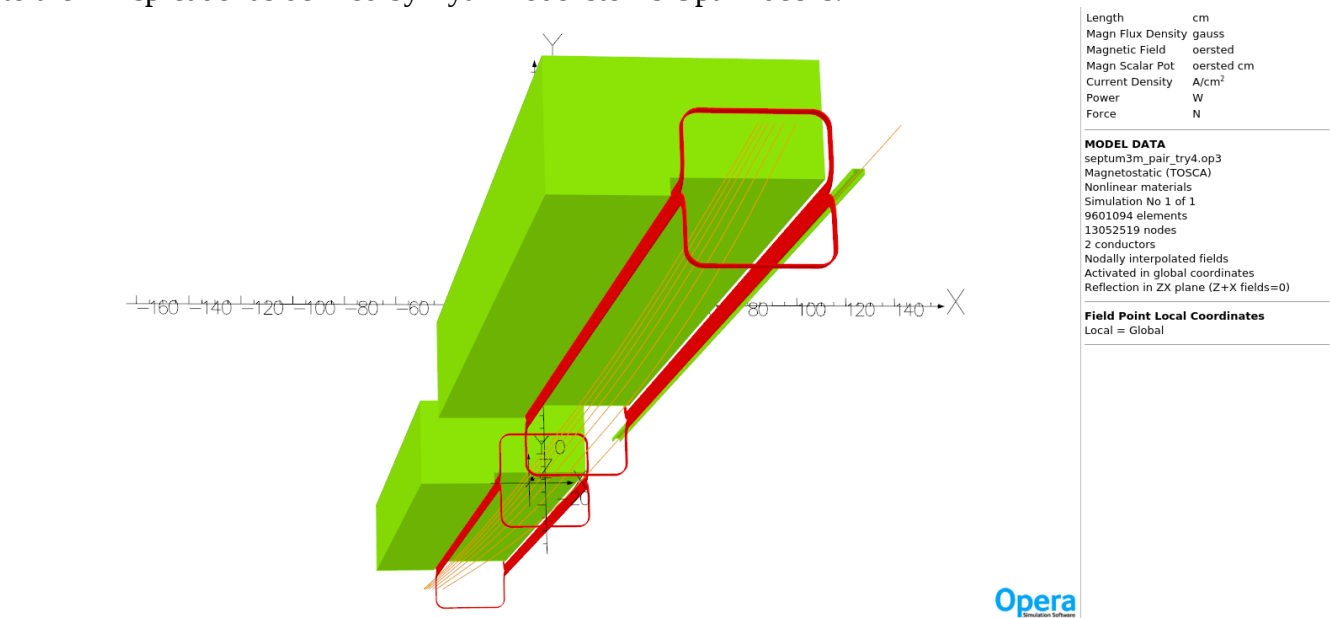


**Second attempt at a conductively-cooled superconducting septum magnet for the FFA upgrade**  
**Jay Benesch**  
**19 August 2022**

NE spreader

The NE and SW spreaders may have different offsets of the second magnet to accommodate the reduced beam spacing in the latter due to higher fourth pass energy. The images in this section pertain to the NE spreader as defined by Ryan Bodenstein's Optim decks.



**Figure 2.** Perspective view of two-magnet system. Beams enter at the back and move towards the viewer. The forward magnet is offset 6 cm to the left so the fourth pass beam passes through the steel tube at right, reducing the stray field it sees. The other six passes see both magnets.

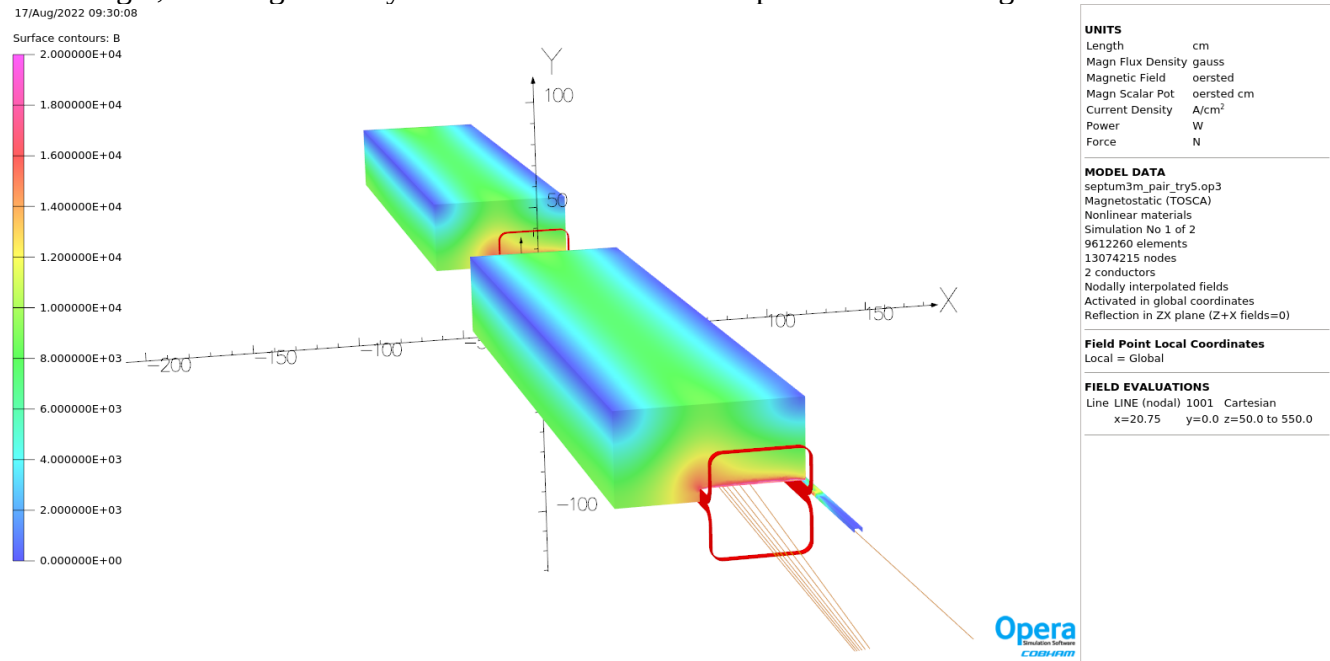


**Figure 3.** Similar view with fields on the surface displayed with color codes at left.

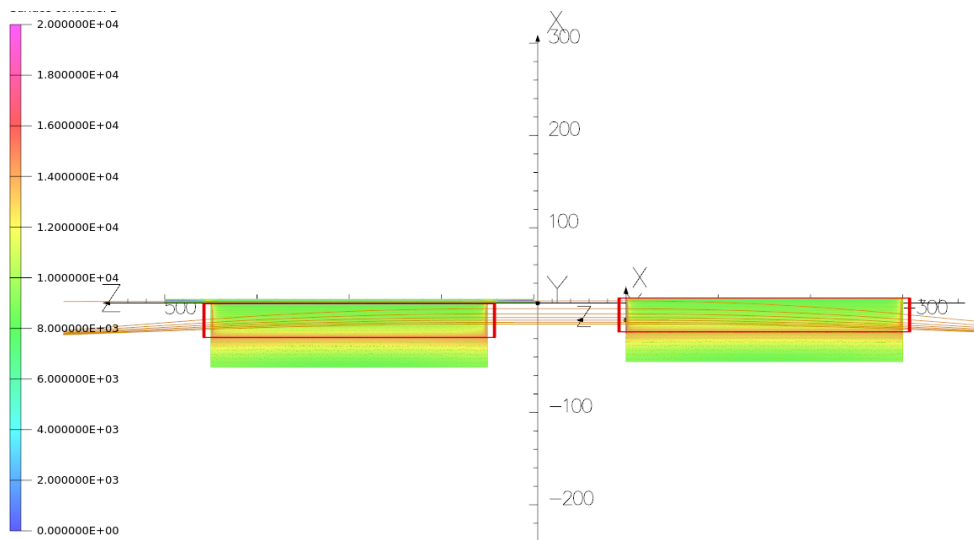


**Figure 4.** Bottom view, surface fields displayed, not perspective

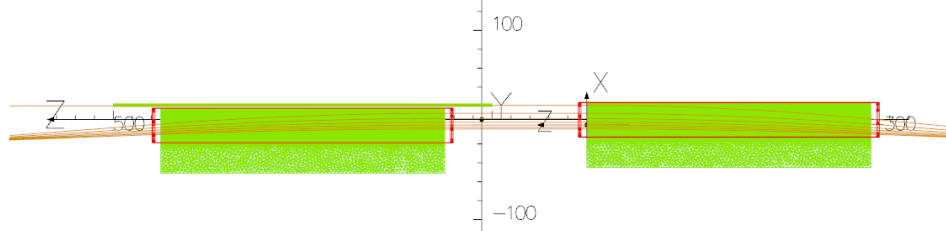


**Figure 5.** Seven orbits through the pair, beams move right to left.

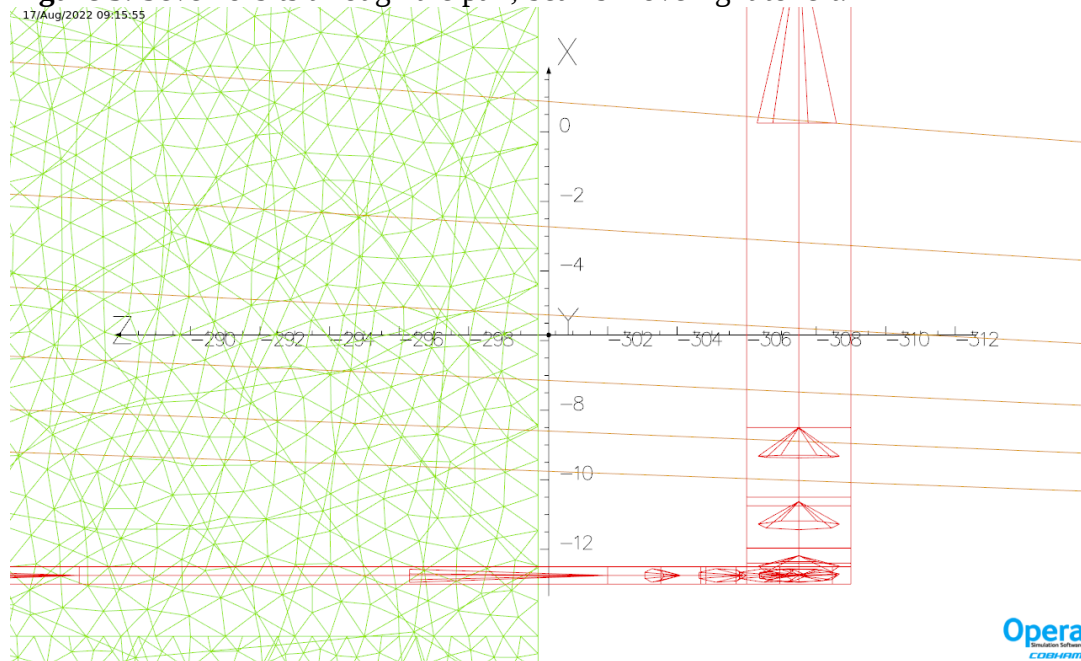


**Figure 6** Five beams entering the upstream magnet. Launch point 89 cm upstream of this magnet. Zoomed in to show proximity of highest energy beam to 5 mm wide coil, ~28 mm.

Length	cm
Magn Flux Density	gauss
Magnetic Field	oersted
Magn Scalar Pot	oersted cm
Current Density	A/cm <sup>2</sup>
Power	W
Force	N

**MODEL DATA**  
septum3m\_pair\_try5.op3  
Magnetostatic (TOSCA)  
Nonlinear materials  
Simulation No 1 of 2  
9612260 elements  
13074215 nodes  
2 conductors  
Nodally interpolated fields  
Activated in global coordinates  
Reflection in ZX plane (Z+X fields=0)

**Field Point Local Coordinates**  
Local = Global

**FIELD EVALUATIONS**  
Line LINE (nodal) 1001 Cartesian  
x=20.75 y=0.0 z=50.0 to 550.0

**MODEL DATA**  
septum3m\_pair\_try5.op3  
Magnetostatic (TOSCA)  
Nonlinear materials  
Simulation No 1 of 2  
9612260 elements  
13074215 nodes  
2 conductors  
Nodally interpolated fields  
Activated in global coordinates  
Reflection in ZX plane (Z+X fields=0)

**Field Point Local Coordinates**  
Local = Global

<b>UNITS</b>	
Length	cm
Magn Flux Density	gauss
Magnetic Field	oersted
Magn Scalar Pot	oersted cm
Current Density	A/cm <sup>2</sup>
Power	W
Force	N

**MODEL DATA**  
septum3m\_pair\_try5.op3  
Magnetostatic (TOSCA)  
Nonlinear materials  
Simulation No 1 of 2  
9612260 elements  
13074215 nodes  
2 conductors  
Nodally interpolated fields  
Activated in global coordinates  
Reflection in ZX plane (Z+X fields=0)

**Field Point Local Coordinates**  
Local = Global

**Opera**  
Simulation Software  
COBHAM

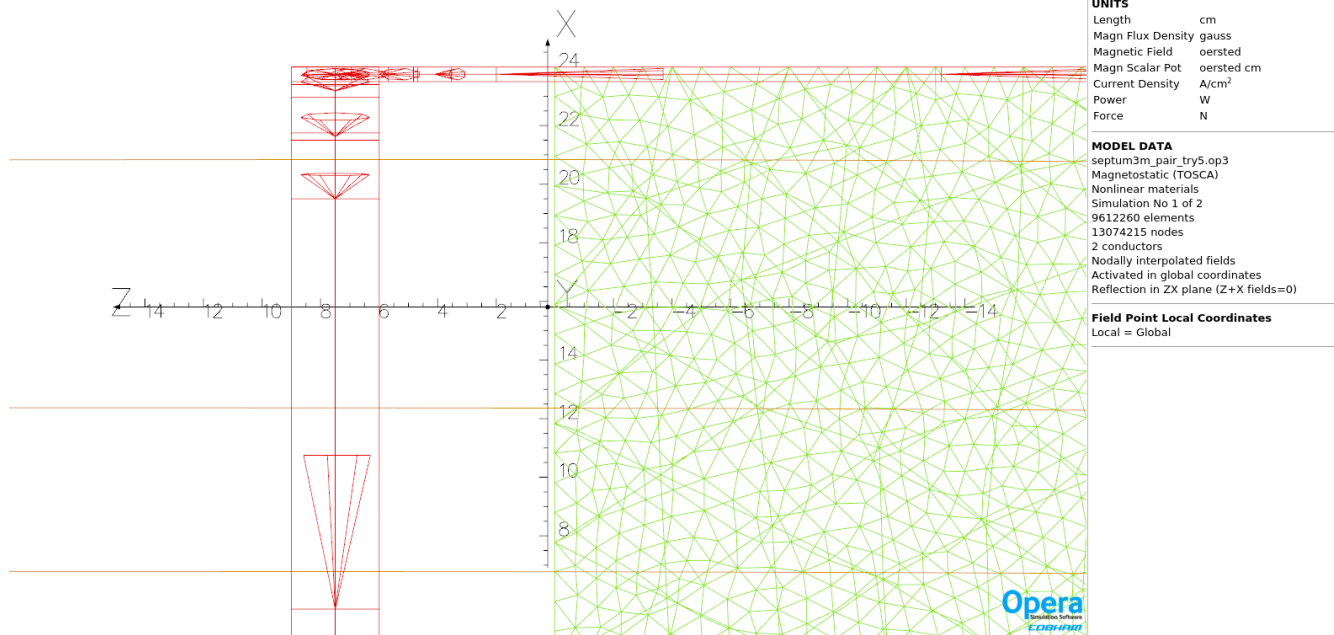


**Figure 7** Top three beams exiting the first magnet in the pair. Top beam is again ~28 mm from the 5 mm wide coil.

17/Aug/2022 09:18:36

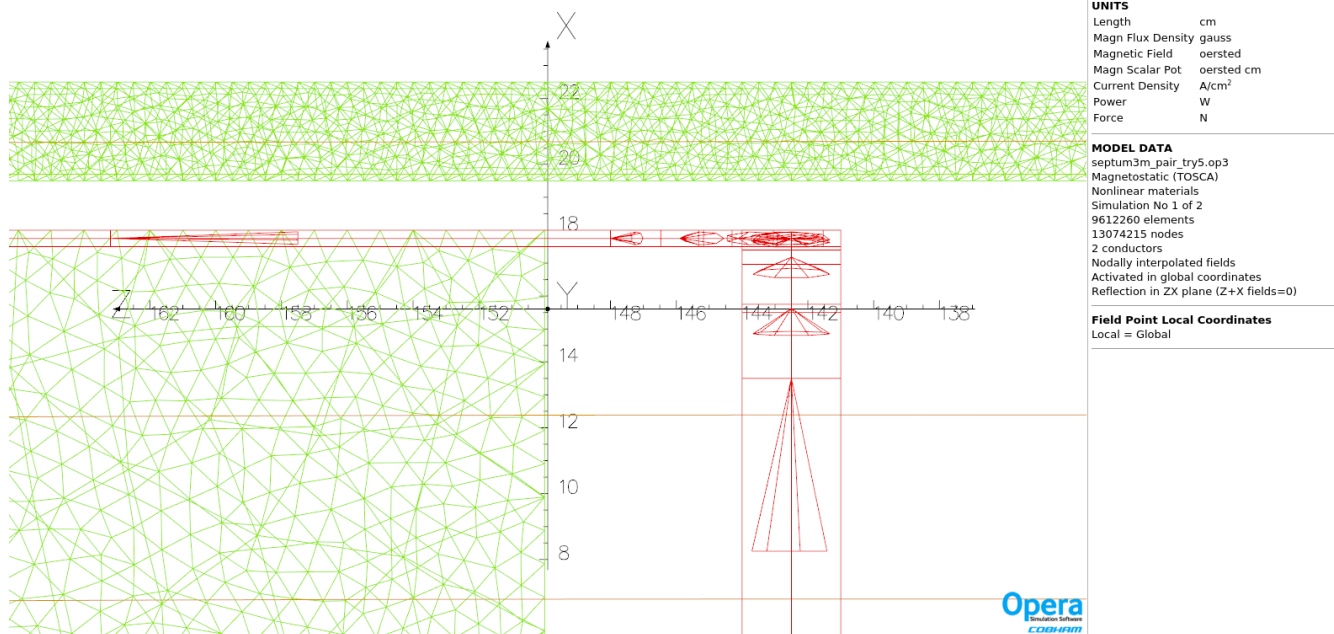


**Figure 8** Top three beams entering the second magnet. Here there's ~30 mm between beam and coil. There is sufficient clearance on the top beam within the second magnet that it can be shifted down 10 mm to make both clearances ~40 mm. The green at the top is a 2 mm wall, 30 mm square (outside) steel tube to shield the passing beam. Recall that the second magnet was shifted 6 cm with respect to the first; 7 cm is more appropriate. The zero of this model is 23 cm above the linac nominal. The steel extends to -51 cm so there is more than ample room to mount it to the floor. Looking at Figure 3, one might extend the steel to -55 cm to reduce saturation.

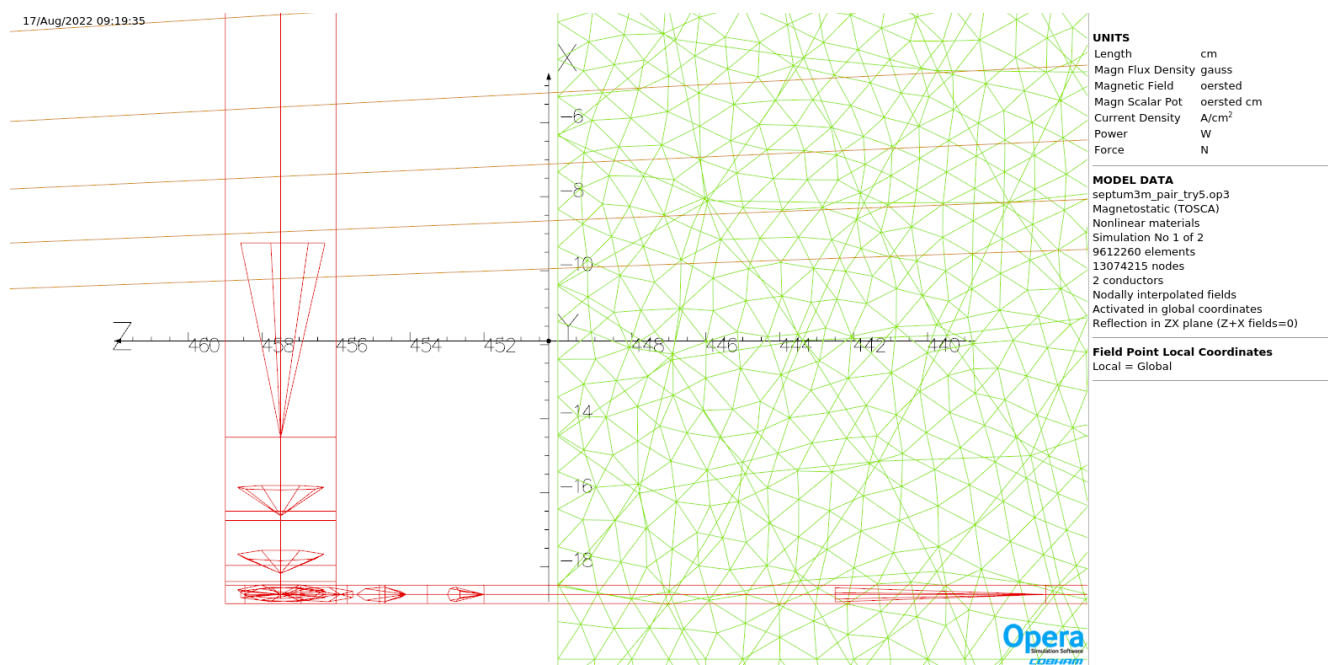


**Figure 9** Beams exiting the second magnet. Again, more than enough clearance to shift it down.  
field on recirculated beam

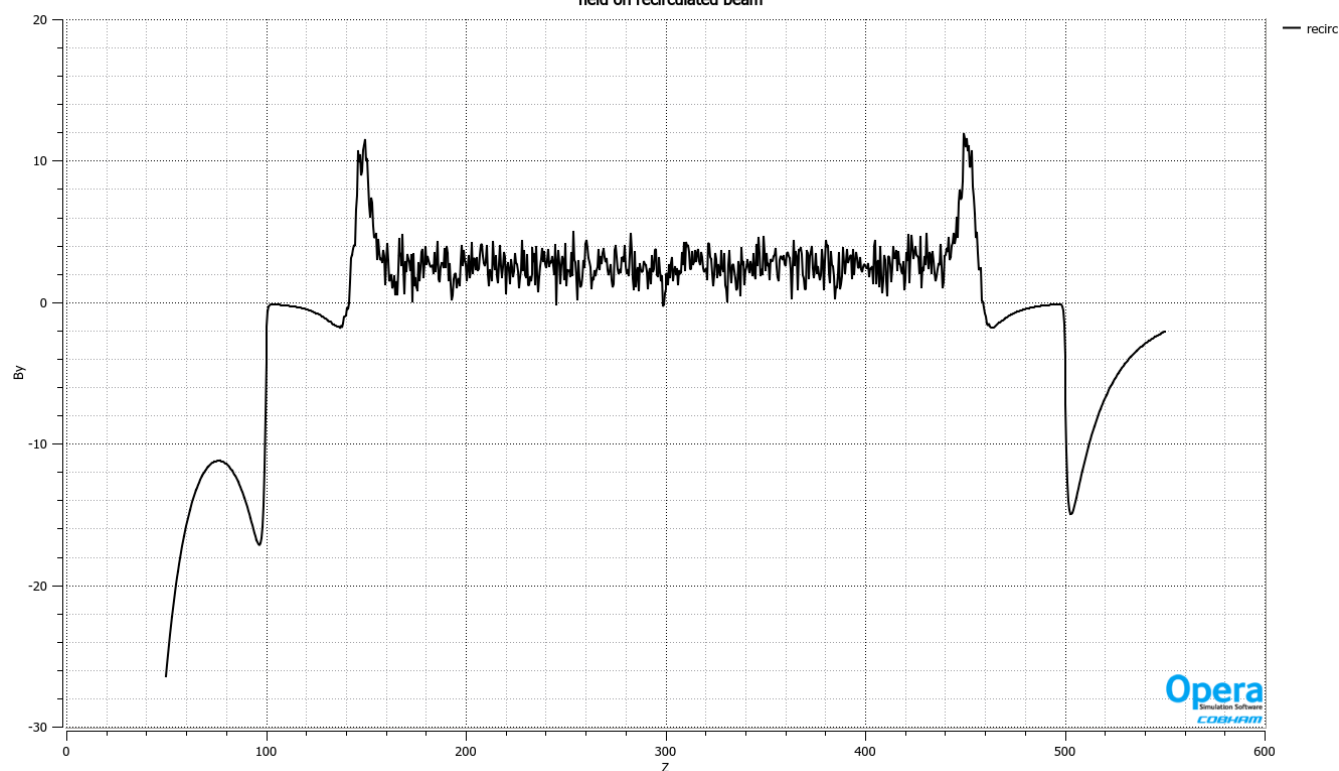


**Figure 10.** Field along the beam passing by the second magnet within the steel shield tube. The tube extends 50 cm beyond the magnet steel on each end. The plot extends 100 cm beyond the magnet steel on each end.



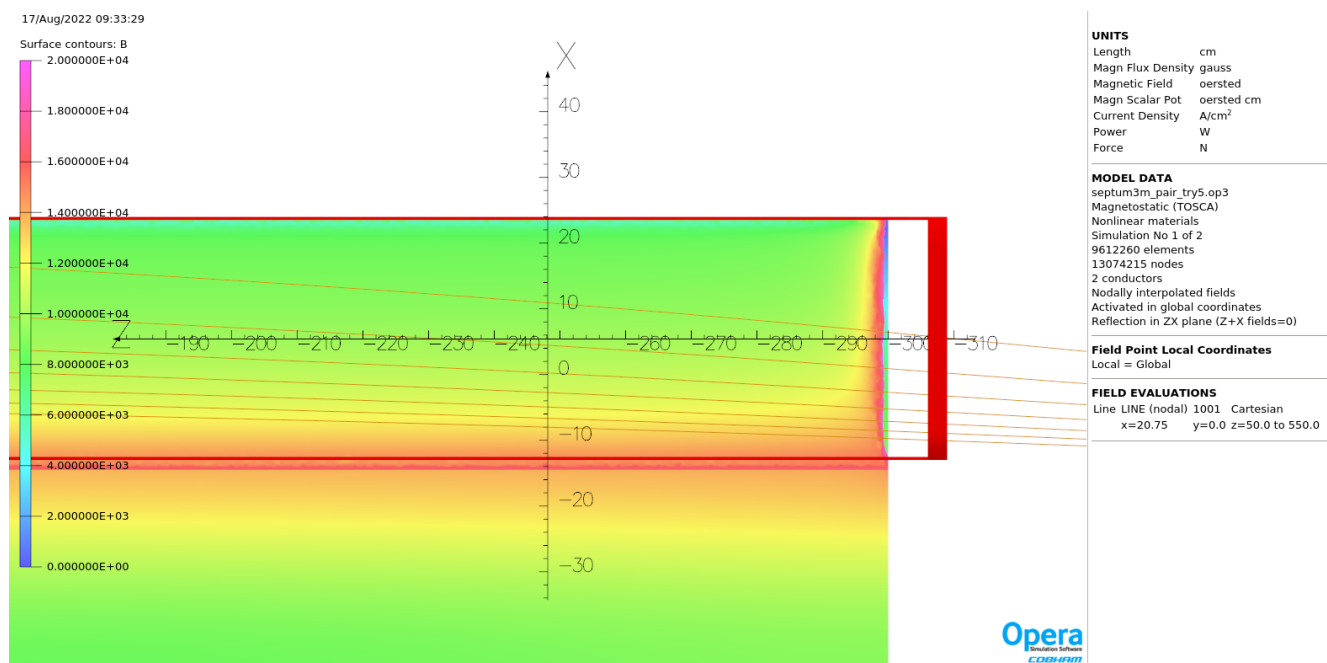


**Figure 11.** Field on the surface of the first magnet with all seven orbits shown. If one looks carefully one sees color gradients at the entrance to the pole. The field at the edge of the steel is above 20 kG so the edge is not shown in the image.

These models were built with maximum voxel size in the beam region 0.5 cm. This is insufficient to get good values for Fourier harmonics along these orbits. This model took about six hours to solve. A model with 0.25 cm maximum voxels in the beam region was prepared and took 28 hours to solve. Harmonics were calculated along the orbits in that model. They will appear better than the harmonics from a model with curved steel and coil as the beams will be closer to the interface in that case. Table 3 of TN-22-010 <https://jlabdoc.jlab.org/docushare/dsweb/Get/Document-254194/22-010.pdf> has harmonics of the YR model with added steel to approximate the required FFA septum.

## Coil and Conductor

There are 61650 AT in the two bedsteads. It is expected that the coil will be fabricated as a single bedstead but modeling that would require eliminating a symmetry which reduces the solution time and was not done. Coil block is 5 mm wide by 60 mm high in the model. My thought was to have a thin aluminum channel extruded and bent to the required shape, 1 mm section with 5.5 mm side lips. Six layers of 1 mm conductor, 60 turns per layer, hexagonal close pack, would be wound into the channel, 360 turns total. Perhaps another aluminum plate to close the box, 0.5 or 1 mm, for better conductive cooling. Current is then 171.25 A. Field at conductor 1.05 T. MgB<sub>2</sub> is suggested based on Akira Yamamoto and Amalia Ballarino, *Advances in MgB<sub>2</sub> Superconductor Applications for Particle Accelerators*, <https://arxiv.org/abs/2201.09501> MgB<sub>2</sub> can sustain this load at 20 K so the task of the cryostat and cryocoolers is less. NbTi is also possible but dealing with the heat load including the leads will be more difficult. Nb<sub>3</sub>Sn wind and react is also an option with copper channel (closer to Nb<sub>3</sub>Sn thermal expansion during reaction cycle than aluminum). It may be desirable to use a coil of eight layers, 480 turns, 128.44 A; I haven't looked at beam clearances for 7 mm or 9 mm coil pack width. The concept allows at least 15 mm clearance on all sides of the 5 mm coil for the cryostat. This model has 90 mm pole gap, 10 mm more than the gap used in TN-22-033. J increased from 180 to 205.5 A/mm<sup>2</sup> 14.2% versus 12.5% on geometry. I am reluctant to increase the gap further to accommodate a larger cryostat section at this stage in the design. Turns per layer can be decreased to get more space if

eight layers are used and the coil is expanded towards the six-beam grouping. (Yes, I recognize this paragraph does not proceed in the most readable fashion, but that's the way my mind worked when I was writing it. Deal with it.)

### SW Spreader

The plots which follow for the SW spreader use the same basic model. Orbits are from the latest version of the spreader obtained from Ryan Bodenstein, with 92 cm drift from second BCOM to this pair.

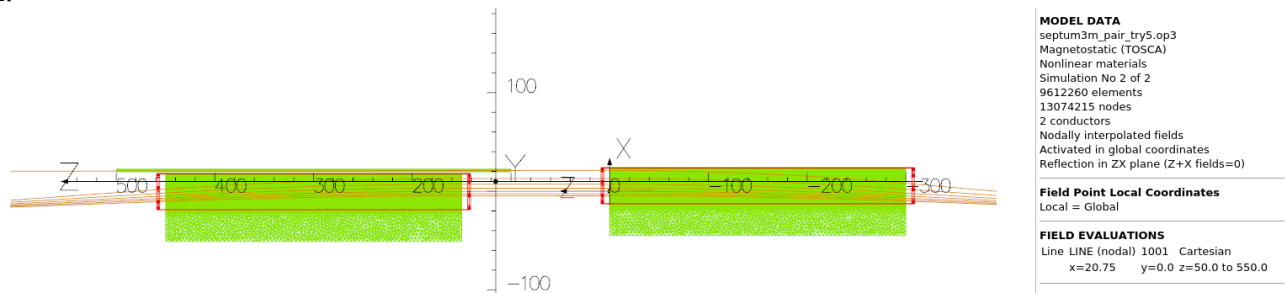


**Figure 12.** Seven orbits through the model, J 212.5 A/mm<sup>2</sup> vs 205.5 A/mm<sup>2</sup> for NE spreader

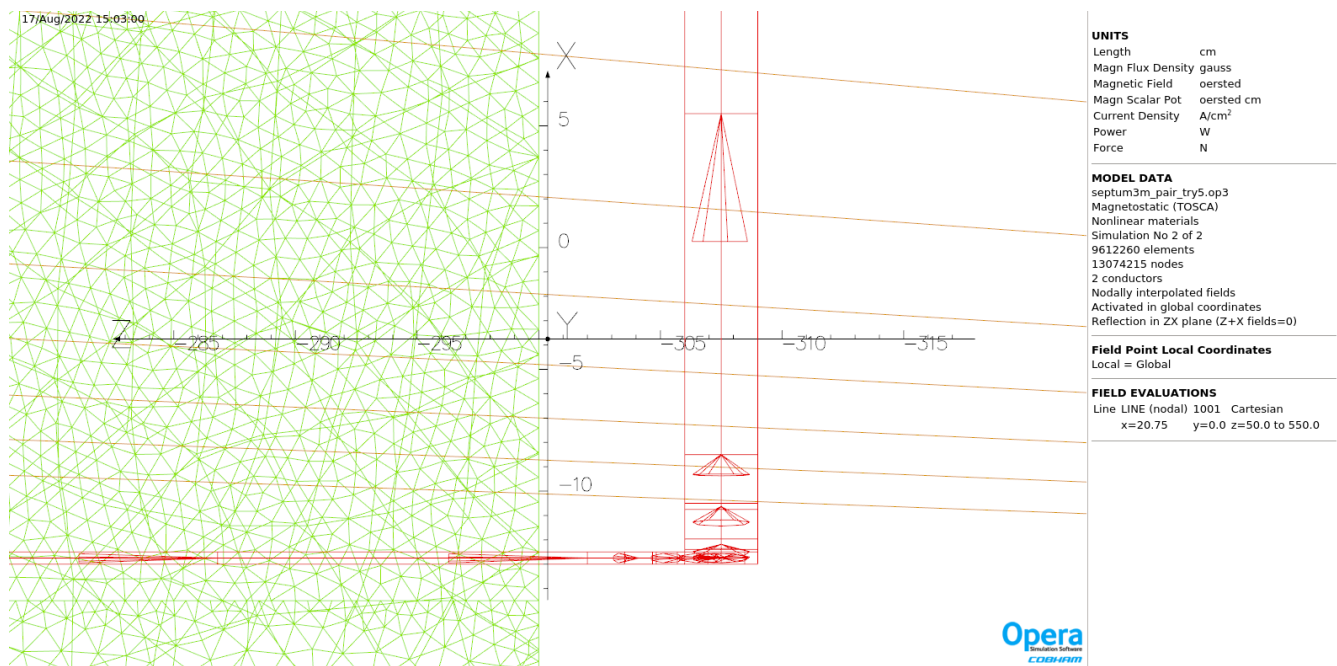


**Figure 13.** Orbits at entrance of model. Clearance of highest energy beam is ~26 mm.

17/Aug/2022 15:03:48

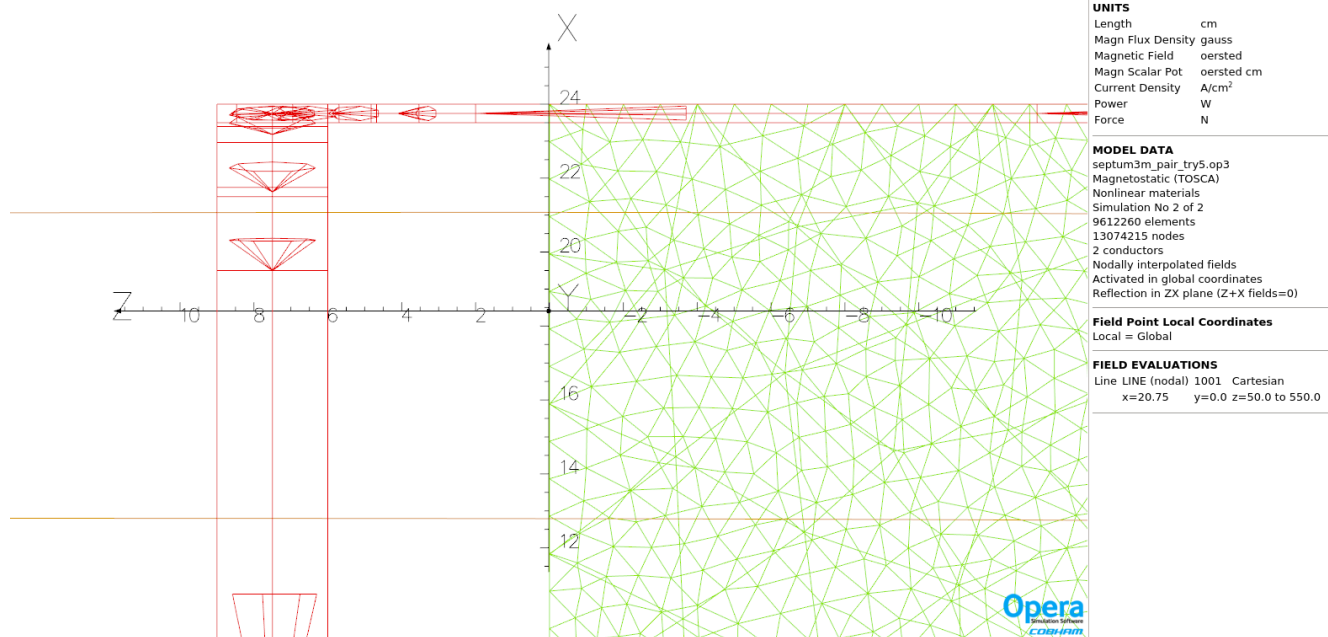


**Figure 14.** Top two beams at exit of first magnet. Again, clearance ~26 mm.

17/Aug/2022 15:04:55

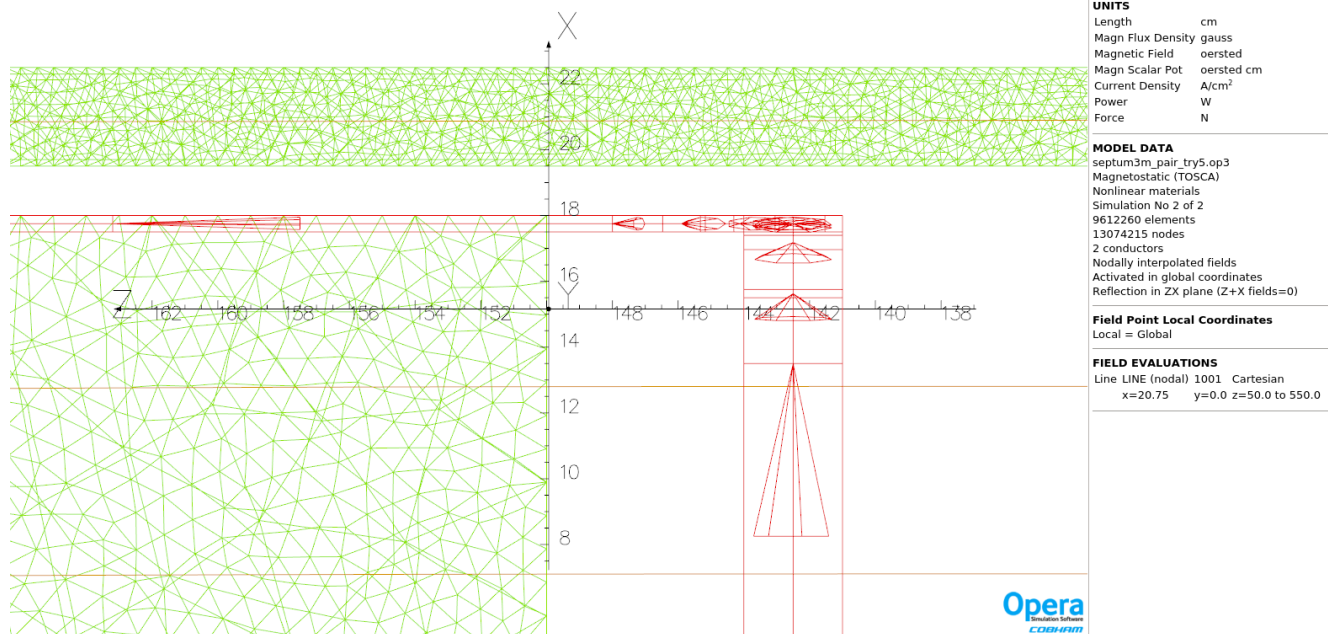


**Figure 15** As in NE spreader, clearances are uneven at the entrance to the second magnet so a downward shift of the second magnet by 10 mm can be done.



17/Aug/2022 15:05:52

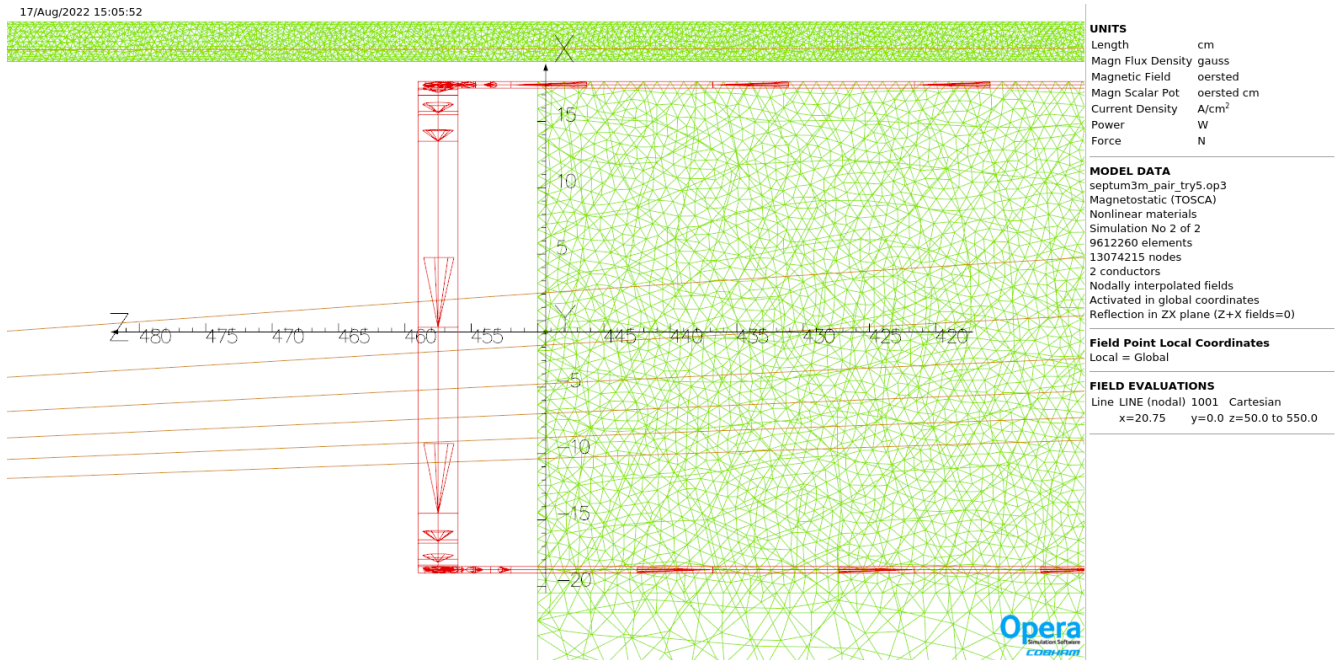


**Figure 16.** Seven beams exiting second magnet, including one in the shield tube. Moving the magnet down 10 mm will not be an issue.

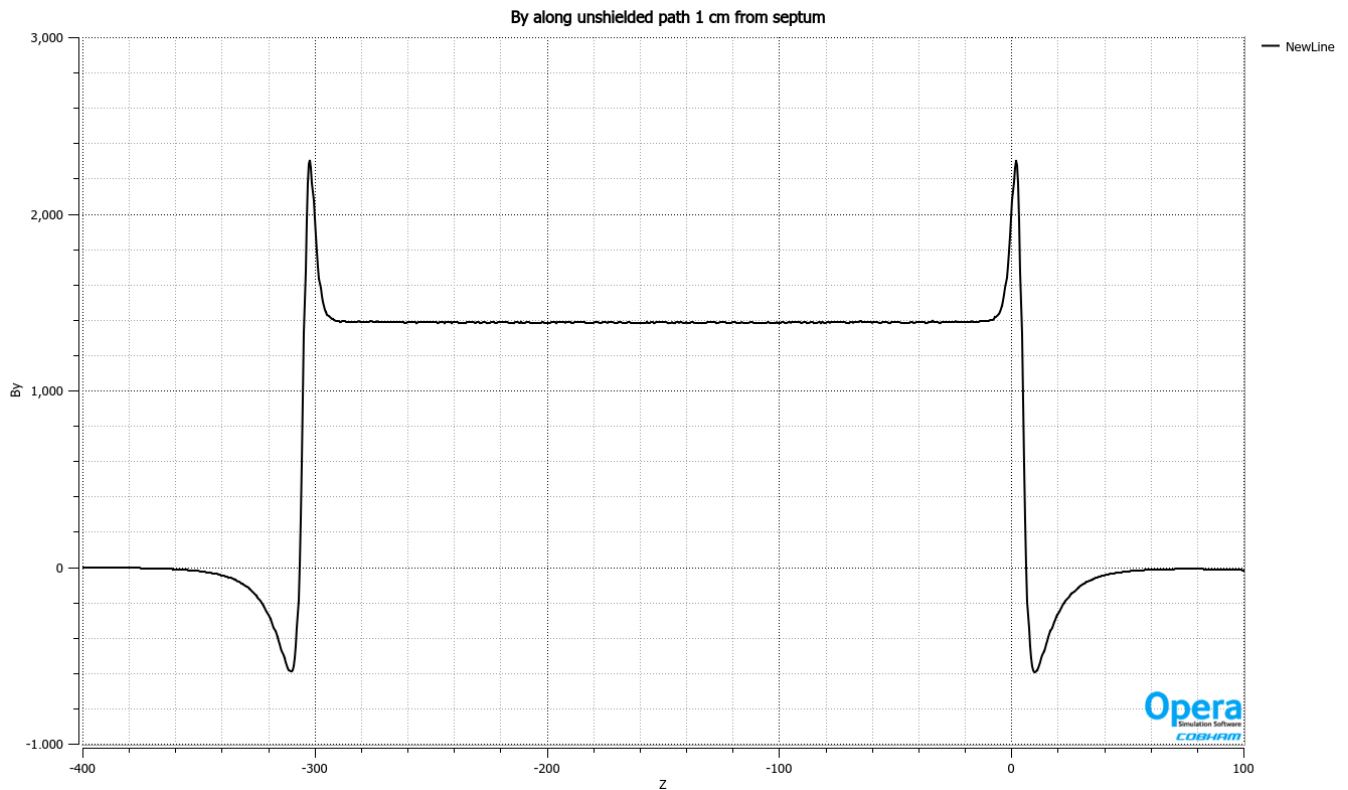


**Figure 17.** Field 1cm from the septum in the first dipole. Clearly the steel tube shown along the second magnet is necessary.

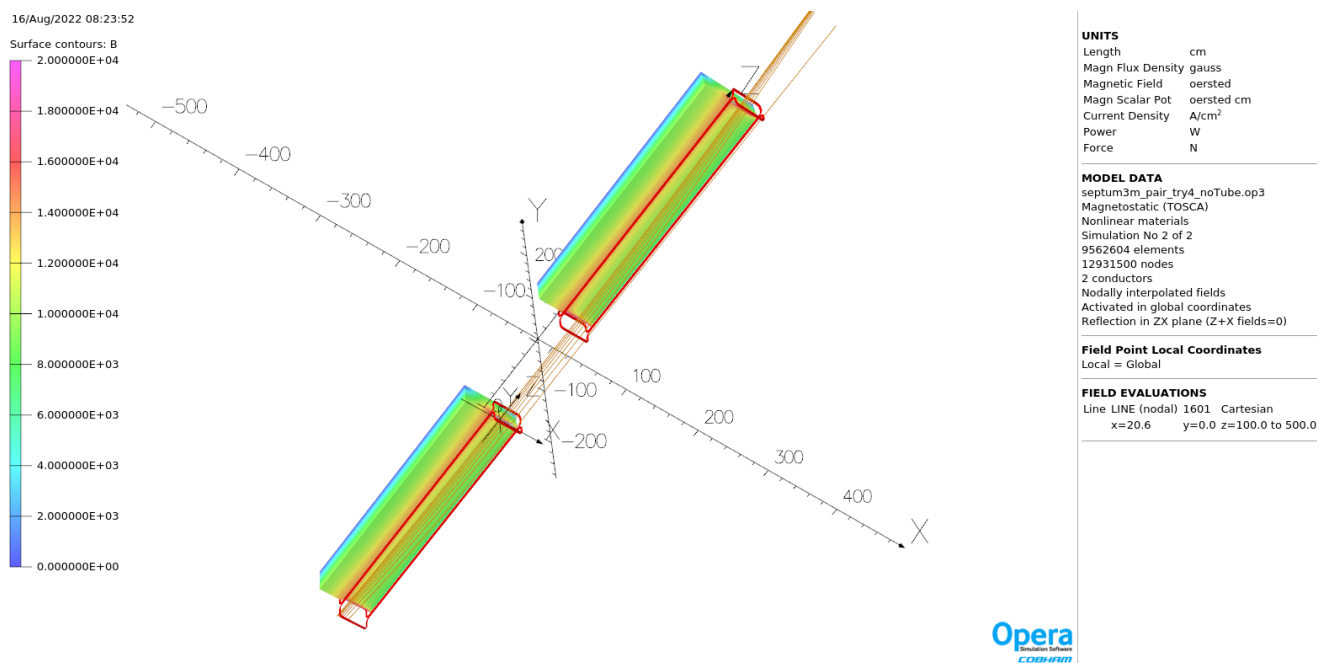


**Figure 18** Perspective view of the model with seven orbits,  $|B|$  on the surface.

## Next steps

1. Convince FFA working group that the upgrade should stop with the 21550 MeV nominal orbit in the NE spreader, aka  $\sim 21$  GeV to Hall D after synchrotron radiation, rather than continuing for another pass. If the 22650 MeV beam, the lowest in Fig. 13, did not exist the clearances in Fig. 13 and 14 could be increased and expanding the coil by 3 mm to lower current (raise turn count) would not be an issue. See bottom of next page.
2. Increase return steel section by 4 cm to reduce saturation.
3. Model with second dipole in set offset by 7 cm versus 6 cm here. Adjust SW launch points if decision in (1) is favorable.
4. When launch points with beam energies including SR radiation losses are available, calculate Fourier harmonics again.
5. Think about chamfering the entry at the first magnet and exit of the second by perhaps 10 cm, returning to steel shown 100 cm from the end. This would help engineering layout. It will make the magnetic modeling much more painful because the conductors will have to be made of bricks and arcs and the ends matched to microns. This will not be started until there is a first engineering layout. This will increase harmonic content, as in the YR, and so should be done only if necessary.

## Conclusions

A more realistic septum arrangement for the NE and SW spreaders has been modeled. Next steps have been outlined. Others need to start thinking about the cryostat design including current lead heat stationing and cryocooler interface. Fourier harmonics along the beam paths shown are given on the next page.

### Fourier harmonics along orbits in each spreader. Gauss at r=1 cm, integrated along full orbit

energy (MeV)	Cos0	Cos1	Cos2	Cos3	Cos4	Cos5	Cos6	Cos7	Cos8	Cos9
8350	-2716152	-24494	-7500	-1304	-91	22.4	6.7	1.4	-1.5	0.2
10550	-5362716	-5661	-1981	-438	-74	-8.4	-3.3	0.0	-1.6	0.0
12750	-5354053	73	-65	-4	-5	0.0	-1.5	0.0	-0.6	0.1
14950	-5354177	594	-194	45	-9	1.2	-1.4	-0.2	-0.8	0.1
17150	-5356370	2346	-797	175	-30	3.7	-2.1	0.2	-1.1	0.1
19350	-5363058	7033	-2321	485	-73	6.6	-2.9	-0.1	-1.7	0.3
21550	-5377857	16805	-5313	1016	-115	-1.3	0.6	-0.6	-1.5	-0.1

energy (MeV)	Cos0	Cos1	Cos2	Cos3	Cos4	Cos5	Cos6	Cos7	Cos8	Cos9
9450	-2816455	-30847	-9241	-1501	-61	41.4	11.0	2.3	-1.4	-0.1
11650	-5547028	-8009	-2770	-606	-98	-11.0	-3.3	-0.5	-1.5	-0.4
13850	-5535214	20	-65	-10	-6	-0.3	-1.5	0.0	-0.8	0.2
16050	-5535291	472	-152	36	-8	1.0	-1.7	0.1	-0.7	-0.1
18250	-5537601	2281	-779	172	-29	3.8	-2.1	0.2	-1.3	0.2
20450	-5546071	8141	-2677	557	-83	7.3	-2.8	0.2	-1.7	0.0
22650	-5567922	22305	-6893	1244	-111	-13.7	4.1	-2.0	-1.4	0.0

Harmonics for the lowest energies include only the orbit through Z=99 cm because the 1 cm radius circles intercepted the steel tube thereafter. Given Fig. 10, the contribution is small. Proximity to the coils at entry and exit clearly matter. Canting the magnets so the beam are farther from the coils at entrance and exit, as in Figure 1, would help. If the septum coil and the steel are radiused as in the ZAs much of the resulting improvement would be lost. Perhaps less loss with chamfer.

### Energy loss, Emittance Dilution (7-pass FFAs)

	E [GeV]	$\rho$ [m]	$\Delta E$ [MeV]	$\langle H \rangle$ [m]	$\overset{rms}{\Delta \epsilon}_N$ [m rad]	$\overset{rms}{\Delta \sigma}_{\Delta E/E}$	$\sigma$ [mm]	
6 passes	FFA 9	10.43	70.6	7	4.0E-03	1.9E-05	3.2E-04	0.6
	FFA 10	11.51	70.6	11	4.0E-03	1.9E-05	3.7E-04	0.7
	FFA 11	12.59	70.6	16	4.0E-03	2.0E-05	4.3E-04	0.8
	FFA 12	13.67	70.6	22	4.0E-03	2.1E-05	5.1E-04	0.9
	FFA 13	14.73	70.6	30	4.0E-03	2.2E-05	6.1E-04	1.1
	FFA 14	15.80	70.6	39	4.0E-03	2.3E-05	7.2E-04	1.3
	FFA 15	16.85	70.6	50	4.0E-03	2.5E-05	8.5E-04	1.5
	FFA 16	17.89	70.6	64	4.0E-03	2.9E-05	1.0E-03	1.8
	FFA 17	18.91	70.6	80	4.0E-03	3.3E-05	1.2E-03	2.1
	FFA 18	19.92	70.6	99	4.0E-03	4.0E-05	1.4E-03	2.5
	FFA 19	20.91	70.6	120	4.0E-03	4.8E-05	1.6E-03	2.9
	FFA 20	21.88	70.6	144	4.0E-03	6.0E-05	1.9E-03	3.4
	FFA 21	22.83	70.6	170	4.0E-03	7.4E-05	2.2E-03	3.9
	FFA 22	23.75	70.6	199	4.0E-03	9.2E-05	2.5E-03	4.4
Geometric Arc Radius [m]		80.6						

Final Energy [GeV]	24.6
Total Energy Loss [MeV]	1080

Dispersion [m]	1.8
Beampipe Diameter [mm]	22

Slide adapted from Alex Bogacz talk

I (Jay Benesch) assert that energy beyond 20 GeV (FFA18) will be subject to excessive beam loss in Halls A and C arcs. Hall D might allow 21 GeV (FFA19) but 19 GeV (FFA17) is more likely for extraction reasons.

#### ● Synchrotron radiation mitigation in FFAs

- High fill factor (88% space filled with bends) increases significantly the bend radius,  $\rho$ .
- By virtue of extremely small dispersion and betas, the horizontal emittance dispersion,  $\langle H \rangle$ , is highly suppressed (factor of 50 lower than in a conventional CEBAF arc lattice).

Slide shown by author to August 17, 2022 J/Psi workshop on physics at higher energies at CEBAF. I pointed out the last column and the amount of beam that would be lost even with perfect steering if energies above 20 GeV were attempted to Halls A and C. Hall D requires only 200 nA for the physics proposed so far in the series of five workshops so 21 GeV may be tolerable there. I also emphasized that 630 MeV of the total 1080 MeV lost to synchrotron radiation was in the last four FFAs listed.